FERMILAB-PUB-81-089-E

Submitted to Physical Review

466

Angular distributions and differential ranges of Ba products from the interaction of ^{238}U with 0.8-400 protons

S. Pandian* and N. T. Porile

Department of Chemistry, Purdue University,

W. Lafayette, Indiana 47907

Angular distributions and differential ranges at 90° to the beam of ^{128}Ba, ^{131}Ba, $^{135}Ba^{m}$ and ^{140}Ba emitted in the interaction of ^{238}U with 0.8-400 GeV protons have been measured. The angular distributions of ^{128}Ba and ^{131}Ba change from forward-peaked to sideward-peaked between 3 and 11.5 GeV, while those of $^{135}Ba^{m}$ and ^{140}Ba are sideward peaked and independent of bombarding energy in the above regime. Momentum distributions of all products are Gaussian at 0.8 GeV with a mean value increasing from 120 $(MeV \cdot A)^{\frac{1}{2}}$ for ^{128}Ba to 139 $(MeV \cdot A)^{\frac{1}{2}}$ for ^{140}Ba. The momenta of the neutron-deficient products decrease by nearly a factor of two with increasing proton energy and the distributions broaden and become asymmetric. On the other hand, the momentum distributions of $^{135}Ba^{m}$ and ^{140}Ba are independent of proton energy. The results are analyzed with the two-step model and compared with the kinematics of the coherent interaction model. The implications of the results and comparisons for the reaction mechanism are considered.

NUCLEAR REACTIONS $^{238}U(p,X)$ ^{128}Ba, ^{131}Ba, $^{135}Ba^{m}$, ^{140}Ba. T_p=0.8-400 GeV. Measured angular distributions and differential ranges at 90° to the beam, deduced two-step model parameters.

PACS 25.40.Rb

*Present address: School of Medicine, Washington University, St. Louis, MO.

I. Introduction

One of the most interesting new results to emerge from the study of high-energy nuclear reactions is the discovery of a change in the dynamic properties of the products of highly inelastic interactions of heavy elements with protons. This change, which is observed at a proton energy of approximately 3 GeV, consists of a relatively sharp peak in F/B, the ratio of forward to backward emission,[1-5] and of a concomitant change in angular distribution from forward-peaked to sideward peaked.[6-10] In addition, the mean ranges and kinetic energies of most of the products exhibiting this behavior decrease markedly over an interval of several GeV centered at this energy,[1,3-5] while the spectra concomitantly broaden.[8,9,11] This behavior has been observed for a number of deep spallation and fragmentation products. The highly inelastic nature of the interactions leading to the formation of these products is attested to by the observation that their excitation functions increase up to an energy of at least 5 to 10 GeV.[3,5] This is in contrast to the behavior exhibited by products of less violent interactions, e.g. fission and spallation, whose excitation functions decrease or are constant in this energy regime.

Additional changes in the dynamic properties of products of highly inelastic interactions have recently been observed at 400 GeV. The angular distributions of some of these products thus show that the differential cross sections for emission at backward laboratory angles are greater than the values at the corresponding forward angles.[10,12] However, differential ranges of Sc nuclides from ^{238}U bombardment are consistent with emission from a residual nucleus that is slowly moving along the beam direction.[13]

These results have been interpreted in terms of a change in the mechanism of highly inelastic proton-nucleus interactions.[5,14,15] For incident proton energies up to approximately 3 GeV, the results are generally consistent with the two-step model. This well tested and generally valid model postulates a temporal separation of the reaction into a prompt intranuclear cascade followed by a slower deexcitation step. The first step consists of a series of quasi-free nucleon-nucleon collisions while in the second step the residual nucleus deexcites by particle evaporation and may, in addition, undergo fission. In view of the steeply rising excitation functions displayed by the products in question, the excitation energy of the residual nucleus is expected to increase with bombarding energy.[16] Since the longitudinal momentum transfer to the struck nucleus has been shown to be proportional to the excitation energy,[17] the forward component of momentum of the residual nucleus also increases with proton energy. As a result, the F/B values of the products of interest should increase with bombarding energy and the angular distributions should become increasingly forward peaked. This is precisely the situation observed up to 3 GeV. If this model were to retain its validity at higher energies, a bombarding energy should eventually be attained at which the optimum excitation energy required to form the product in question is transferred to the struck nucleus. At this point, the excitation energy transfer should become essentially independent of bombarding energy. In this situation, the momentum imparted to the struck nucleus becomes proportional to the ratio of the momentum of the incident proton to its kinetic energy. As long as the incident proton is not fully relativistic, these quantities are inversely related and so F/B should decrease. However,

once the incident proton becomes fully relativistic this ratio becomes independent of proton energy and so F/B should level off. Scheidemann and Porile[3] calculated the energy dependence of F/B of a number of fragmentation and deep spallation products on the basis of the two-step model. While the calculation was able to account for the variation of F/B with energy up to $\sim$ 4 GeV, it could not account for the continuing decrease in this quantity observed at higher energies.

A possible explanation for the phenomena observed above 3 GeV has been advanced[5,14] on the basis of the coherent interaction model.[18,19] According to this model, an ultra-relativistic hadron ($\beta \sim 1$) interacts coherently with an effective target comprised of the nucleons lying in its path, instead of with individual nucleons. The collective interaction results from the longitudinal Lorentz contraction of the nucleus as seen by the projectile. The result of this interaction is the formation of an excited hadronic state which, due to relativistic time dilation, is ejected from the nucleus prior to its decay to the final multi-particle state. The nucleons involved in this coherent process thus do not participate in the intranuclear cascade as evidenced, for instance, by the fact that the multiplicity of charged particles emitted at small angles in a hadron-nucleus interaction is independent of target A.[20,21] Further evidence for coherent hadron-nucleus interactions has been obtained from the unusual dependence on target A of the inclusive particle production spectra at large transverse momenta ($Ed^3\sigma/dp^3 \propto A^{\alpha}$, where $\alpha > 1$).[22] Furthermore, it has been shown[23] that the coherent interaction model may already be valid at an energy of a few GeV, i.e. in the energy regime where the observed changes in recoil properties occur.

It has been conjectured[5,14] that the ejection of a tube-like aggregate of nucleons at forward angles, coupled with possible additional mass loss from the surface of the resulting "tunnel", results in a highly unstable residual nucleus. If breakup occurs prior to relaxation, and recent differential range and angular distribution measurements indicate that this is the case,[10,13] the resulting fragments should be preferentially ejected transversely to the beam direction. Furthermore, since the interaction of the incident proton is localized and since the nucleons participating in this interaction do not cascade, relatively little energy and momentum are transferred to the spectator remnant. The angular distributions of the fragments resulting from the breakup of this remnant should thus peak at 90^{o} and be essentially symmetric about this angle in the laboratory system, while the F/B ratios should be close to unity. As indicated above, these are precisely the results obtained in recent experiments.

Although the coherent interaction model appears to offer an explanation of the observed phenomena, there are some major problems with this approach. Both differential range studies[11] and coincidence measurements[14] on fragments emitted in the interaction of ^{238}U with high-energy protons indicate that extensive mass loss occurs prior to breakup. It is difficult to see how this can occur without significant momentum transfer. This difficulty may be an indication of the possible occurrence of various unusual phenomena that have received serious attention in recent years. A near-central collision of an ultra-relativisitic hadron with a heavy nucleus may thus trigger the formation of a pion condensate,[24] and lead to the formation of abnormally dense nuclear matter.[25,26] It has been pointed out[27] that pion condensation can

induce the occurrence of a shock wave, a phenomenon expected to result in angular distributions peaking at sideward angles.[28] Whatever the details of the mechanism, pion condensation, if it occurs, should greatly influence the dynamics of proton-nucleus interactions.

It is clear that a definitive explanation must await the results of more detailed experiments. Furthermore, although we have summarized above what we believe to be the essence of the observed changes, this summary is actually based on rather fragmentary evidence. The only relatively complete set of data covering the GeV energy regime, i.e. excitation functions, recoil properties, angular distributions, and spectra, has thus been obtained for Sc fragments formed in the interaction of ^{238}U with protons.[3,7,10-13] It would be of interest to obtain similar data for deep spallation products in order to ascertain that the observed changes in dynamic properties are indeed as general as we suspect they are. We have previously determined the excitation functions and thick-target recoil properties of Ba nuclides formed in the interaction of ^{238}U with high-energy protons[1,5,29] and also measured the angular distributions and differential ranges at 11.5 GeV.[8] We report here the results of differential range and angular distribution measurements performed at 0.8, 3.0, and 400 GeV. Similar measurements have previously been performed at 2.2 GeV.[30,31] The results of these studies should permit us to trace the evolution of the kinematic properties over the entire GeV energy regime.

II. Experimental

The experimental procedure used in this work was similar to that employed in our study of the angular distributions and differential ranges of Sc fragments,[10,11] which should be consulted for complete details.

Briefly, irradiations were performed with 0.8 GeV protons in line B of the Clinton P. Anderson Meson Physics Facility (LAMPF), with 3.0 GeV protons in the internal beam of the zero gradient synchrotron (ZGS), and with 400 GeV protons in the NO beam line at Fermilab.

The experiments involved the irradiation in vacuum of thin UF_4 targets and the collection of the emitted fragments in either aluminum (angular distributions) or Mylar (differential ranges). The targets consisted of 0.1-0.3 mg/cm^2 UF_4 evaporated onto high-purity aluminum (99.999%) and were inclined at 30^o or 150^o (ZGS) and at 45^o or 135^o to the beam. The irradiations ranged in duration from 1 hr (ZGS) to 1 week (Fermilab).

For the angular distribution experiments, the catchers consisted of 20-25 μm thick 99.999% pure aluminum. It was found that these foils were sufficiently thick to stop all Ba fragments. An additional Al foil backed up the catchers in order to protect them from possible fragments originating in the catcher holder. The catchers intercepted the angular ranges of 15^o - 105^o and 75^o - 165^o relative to the beam direction (5^o - 105^o and 75^o - 175^o at Fermilab). Following bombardment, the foils were cut along isotheta lines[32] into 15^o wide strips (a 10^o wide strip was cut at the most forward and backward angles at Fermilab). The solid angle subtended by each catcher as well as the average recoil angle were evaluated with a code[33] which, in addition to the target-catcher geometry, took into account the beam profile at the target location. This profile was determined from the distribution of the ^{24}Na activity in the target backing.

For the differential range experiments, the catchers consisted of up to fourteen 200-300 μg/cm^2 thick Mylar foils. The foils intercepted the angular interval of 75^o - 105^o to the beam (80^o - 100^o at Fermilab). A thick aluminum mask cut along isotheta lines[32] defined these intervals.

Following irradiation, barium was separated from the various foils[8] and the resulting samples were assayed with Ge(Li) spectrometers. Results were obtained for the following nuclides, where the energies in keV of the observed γ-rays are listed in parenthesis: ^{128}Ba(443), ^{131}Ba (123, 496), ^{135}Ba^{m} (268), and ^{140}Ba (537). The counting rates were corrected for radioactive decay and chemical yield. The angular distribution data were further corrected for differences in solid angle, and the forward and backward halves were combined by normalizing them to each other at their common intervals. The differential range data, in turn, were further corrected for the increase in effective catcher thickness resulting from the wide angular acceptance of the catchers, as well as for energy loss in the target and resolution.[11]

Subsidiary blank experiments were performed at all three accelerators to determine whether there was any contribution to the observed activities from extraneous sources. Upper limits of 2% could be set in all cases. The effect of target thickness on the data had been previously investigated in our 11.5 GeV experiment,[8] where it was concluded that scattering effects for targets of comparable thickness were negligible.

III. Results

A. Angular distributions

The angular distributions of ^{128}Ba, ^{131}Ba, and ^{140}Ba are displayed in Figs. 1-3, respectively, as differential cross sections normalized to 4π when integrated over all space. The results for ^{135}Ba^{m} are similar to those obtained for ^{140}Ba but are of lower overall quality. Our previously reported results[8] at 11.5 GeV are included for completeness. The points in the figures represent the average of two or three replicate results obtained at each energy. Typical error bars are shown. They represent the larger of the standard deviations in the mean

values and the estimated uncertainties in the individual determinations. The latter are comprised of the statistical uncertainties in counting rates (2-4%), estimated errors in the determination of solid angles and their dispersion due to finite target size (2-5%), uncertainty in forward-backward normalization (2%), and error in chemical yield determination (2%).

The curves through the points in Figs. 1-3 are the result of a two-step model fit. According to this widely used model, the differential cross section in the laboratory system at angle θ_L is given by the expression[8]

$$F_L(\theta_L)=\frac{1+(b/a)\cos^2[\theta_L+\sin^{-1}(\eta_{\parallel}\sin\theta_L)]}{1+b/3a}$$

$$\times\ \frac{[\eta_{\parallel}\cos\theta_L+(1-\eta_{\parallel}{}^2\sin^2\theta_L)^{1/2}]^2}{(1-\eta_{\parallel}{}^2\sin^2\theta_L)^{1/2}} \qquad (1)$$

The two parameters in this expression are the velocity ratio $\eta_{\parallel}=v_{\parallel}/V$ and the anisotropy parameter b/a. Here $v_{\parallel}$ is the forward component of velocity imparted to the struck nucleus in the initial interaction and V is the velocity acquired by the product as a result of the breakup step. Since the two steps are assumed to be temporally well separated the angular distribution of V in the moving system must be symmetric about 90^o to the beam direction and is assumed to obey the relation

$$F(\theta)=\frac{1+(b/a)\cos^2\theta}{1+b/3a} \qquad (2)$$

More complete details about the assumptions inherent in the use of Eq. (1) have been published elsewhere.[8,10] The parameters derived from the fits to the data are summarized in Table I. It may be noted that,

in general, the two-step model gives a good fit to the data.

An essentially equivalent parametrization of the angular distributions,[10] but one that is independent of any assumed reaction mechanism, is given by the expression

$$F_L(\theta_L)=1+A_1\cos\theta_L+A_2\cos^2\theta_L \qquad (3)$$

The experimental angular distributions, adjusted in intensity to yield $F_L(90^o)=1$, were fitted with Eq. (3) and the resulting values of the coefficients A_1 and A_2 are also listed in Table I.

B. Spectra

The corrected differential ranges were converted to spectra by means of the range-energy tables of Northcliffe and Schilling.[34] Since the data for all the Ba products excepting $^{135}Ba^m$ represent cumulative chain yields the atomic number of these products, which is required to perform this conversion, is not equal to that of Ba. The required values were obtained on the basis of reported charge dispersion data.[29] A small correction (< 2%) was applied to account for the difference between the tabulated path lengths and the experimentally determined projected ranges. The magnitude of this correction was obtained from the calculation by Lindhard, Scharff, and Schiøtt.[35] The results, displayed as momentum spectra, are shown in Figs. 4-7. The uncertainties in the data points are roughly comparable to those in the angular distributions with the exception of an additional uncertainty of about 5% in the range-energy relation. At 0.8 GeV the spectra of all the Ba products appear to be Gaussian and the curves through the points represent the result of a Gaussian fit. This is also the case for ^{140}Ba and $^{135}Ba^m$ at the higher energies. The

spectra of the more neutron deficient products become increasingly asymmetric at the higher energies and the curves through the points are merely meant to accentuate the shape of the spectra. An attempt was made to fit the energy spectra with a smeared Maxwellian distribution, an approach that has been successfully used to systematize the spectra of light fragments.[36] However, reasonable fits could only be obtained in the same instances where the momentum spectra could be fit by Gaussians. The mean momenta and kinetic energies of the products are summarized in Table II. The full widths at half maximum (FWHM) of the momentum distributions are also tabulated. In those instances where Gaussian fits were made, the widths are based on the fits to the data. The differential ranges were also converted to reciprocal velocities and the mean values of the latter were combined with the $\eta_{\parallel}$ derived from the angular distributions to yield $\langle v_{\parallel} \rangle$ by the relation $\langle v_{\parallel} \rangle = \langle \eta_{\parallel} \rangle \langle 1/V \rangle$. The mean forward velocity components of the struck nuclei derived in this fashion according to the two-step model are summarized in Table II.

IV. Discussion

A. Dependence of recoil properties on proton energy and product composition.

The results shown in Figs. 1-7 display some noteworthy trends. The angular distributions of neutron deficient ^{128}Ba and ^{131}Ba become increasingly forward peaked between 0.8 and 3 GeV. Between 3 and 11.5 GeV, the by now well known transition from forward to sideward peaking occurs. At 400 GeV, the peak at sideward angles is somewhat more accentuated and the curves are more nearly symmetric about 90^{o}, although the ratio of forward-to-backward emission remains somewhat larger than unity. By contrast, the angular distribution of neutron excess ^{140}Ba

is sideward peaked, essentially symmetric about 90^{o} at all energies, and appears to be practically independent of bombarding energy. Within somewhat larger limits of error, the angular distributions of $^{135}Ba^{m}$ are qualitatively similar to those of ^{140}Ba.

The momentum distributions also fall into two distinct groups on the basis of product composition. The spectra of ^{128}Ba and ^{131}Ba at 0.8 GeV thus are Gaussian and peak at values in excess of $120(MeV \cdot A)^{\frac{1}{2}}$. With increasing proton energy, the peaks shift to lower values and the curves become increasingly asymmetric. On the other hand, the spectra of $^{135}Ba^{m}$ and ^{140}Ba are invariant Gaussians at all energies.

The above trends are displayed in somewhat different form in Figs. 8-11, which show the energy dependence of the various parameters extracted from the data. The mean momentum and the width of the momentum distribution are plotted in Figs. 8 and 9, respectively. The momenta of ^{140}Ba and $^{135}Ba^{m}$ are approximately 140 and $130(MeV \cdot A)^{\frac{1}{2}}$, the ^{140}Ba distribution being slightly narrower than that of $^{135}Ba^{m}$. These values are consistent with those of colinear fission fragments with comparable mass number resulting from the interaction of ^{238}U with 2.9 GeV protons.[37] This accord indicates that these products are the result of low deposition energy fission over the entire GeV regime of bombarding energies. The slight but systematic difference between the mean momenta, as well as that between the widths of the distributions, is the result of the well established relation between the composition of a fission product of given mass number and the excitation energy transferred to the struck nucleus in the intranuclear cascade. Hogan and Sugarman[38] have shown that there is a nearly linear inverse dependence of the excitation energy on the neutron to proton

ratio of products lying in a narrow mass interval. Since the excitation energy determines the extent of mass and charge dissipation it follows that the more neutron-deficient fragments result from lighter and more broadly dispersed fissioning nuclei. As a result, these products have somewhat broader momentum distributions centered at slightly lower values than more neutron-excess fragments.

The momenta of neutron-deficient ^{128}Ba and ^{131}Ba show a totally different energy dependence. At 0.8 GeV the mean momenta of these products are only slightly lower than those of $^{135}Ba^{m}$ or ^{140}Ba while the widths are only marginally greater. These results indicate that these products are formed in binary fission, albeit higher deposition energy fission than that involved in the formation of neutron-excess products. The dependence of these quantities on fragment composition thus is in line with the above considerations.

The rapid decrease in the momentum of these products between 0.8 and 11.5 GeV and the concomitant broadening of the spectra indicate that a different mechanism begins to dominate in this regime. This statement is buttressed by the fact that the excitation functions of these products rise sharply until $\sim$ 6 GeV.[1,5] The shape of the spectra as well as the reduced magnitude of the mean momentum are indicative of deep spallation, a process in which extensive mass dissipation occurs via emission of nucleons and light fragments. Cumming and collaborators[39,40] have systematized the momenta of spallation and deep spallation products on the basis of a simple model which attributes the fragment momentum to the random addition of the momenta of the emitted particles. The momenta of ^{128}Ba and ^{131}Ba at 11.5 and 400 GeV are consistent with the Cumming systematics, thereby adding confirmatory evidence for a deep spallation mechanism.

The energy dependence of b/a and $\langle v_{\parallel} \rangle$, depicted in Figs. 10 and 11, respectively, provides further evidence for the invariance of the fission process leading to the formation of $^{135}Ba^{m}$ and ^{140}Ba on the one hand, and to the change in the mechanism for the formation of ^{128}Ba and ^{131}Ba on the other. The anisotropy parameter of the neutron-excess fragments is $\sim$-0.2 at all energies, reflecting the essentially uniform sideward peaking observed at GeV energies. Since fission fragment anisotropies reflect preferred emission of fragments in a plane perpendicular to the direction of the angular momentum vector, the angular distribution of the angular momentum vector associated with the intranuclear cascade should play an important role in determining the fragment anisotropies. Crespo. Cumming, and Poskanzer[30] examined the results of the Vegas cascade code[41] for 378 MeV protons on ^{238}U from this point of view. They found that the angular distribution of angular momentum vectors for low deposition energy (E*<50MeV) cascades peaked at 0^{o} and 180^{o} to the beam. The products of such low energy transfers, e.g. ^{140}Ba, should thus have sideward peaked angular distributions. It was pointed out[30] that these low E* interactions appear to be primarily the result of peripheral collisions in which a single nucleon is emitted at forward angles, in accord with the original explanation of negative fission fragment anisotropies by Halpern.[42]

It was further found[30] that the angular distribution of angular momentum vectors becomes isotropic for moderate E* values, and peaks at sideward angles for high E*. This trend suggests that the sideward peaking in the angular distribution of fission products should become less pronounced and should eventually give way to forward-backward peaking in the moving system as the products become increasingly neutron deficient. Such a trend was experimentally observed by Hogan and

Sugarman at 450 MeV.[38] The present b/a values at 0.8 GeV increase as the Ba products become increasingly neutron deficient in agreement with the earlier observations. It does appear, however, that at this higher proton energy, b/a of even highly neutron deficient ^{128}Ba is at most zero, so that positive anisotropies are less likely than they appear to be at lower energies.

The values of $\langle v_{\parallel} \rangle$ at 0.8 GeV are seen to increase as the Ba products become more neutron deficient, a trend that is completely consistent with the other trends at this energy described above. This follows from the fact that in this energy regime $\langle v_{\parallel} \rangle$ is proportional to $\bar{E}^*$, the mean excitation energy transferred to the struck nuclei in the intranuclear cascade.[17] In addition to accounting for the $\langle v_{\parallel} \rangle$ values of all Ba products at 0.8 GeV, the $\langle v_{\parallel} \rangle$-$\bar{E}^*$ relation also accounts for the energy independence of the $\langle v_{\parallel} \rangle$ values of ^{140}Ba and ^{135}Ba^m as well as for their relative magnitude.

The $\langle v_{\parallel} \rangle$ values of ^{128}Ba and ^{131}Ba exhibit a complex dependence on bombarding energy. The increase observed between 0.8 and 3 GeV is readily understandable within the context of the two-step model. In view of the rising excitation functions of these products, the excitation energy of the cascade residues should increase with proton energy.[16] Since $\langle v_{\parallel} \rangle$ and $\bar{E}^*$ are proportional to each other, the observed behavior of $\langle v_{\parallel} \rangle$ follows. The abrupt decrease in $\langle v_{\parallel} \rangle$ observed above 3 GeV cannot be reconciled with the two-step model. At 11.5 and 400 GeV the $\langle v_{\parallel} \rangle$ values become comparable to those associated with the formation of ^{140}Ba and ^{135}Ba^m in spite of the fact that the interactions leading to the neutron deficient products remain considerably more inelastic, as evidenced, for instance, by their much lower momenta. The observed variation of the $\langle v_{\parallel} \rangle$ is qualitatively similar to that previously

derived from thick-target recoil studies[5] and appears to be a general phenomenon for deep spallation and fragmentation products from the interaction of heavy elements with high-energy protons.[1-5,10] It may be noted that as the $\langle v_{\parallel} \rangle$ of ^{128}Ba and ^{131}Ba approach those of ^{140}Ba, the b/a values likewise approach those of the latter. It thus appears that the correlation between these two quantities observed at low energies continues to hold at the higher energies even if they no longer reflect the occurrence of a temporally well separated intranuclear cascade.

B. Comparison with coherent interaction model

As outlined in the Introduction, there is considerable evidence that the intranuclear cascade model ceases to be applicable in near-central collisions of high-energy protons. The experimental data discussed in the preceeding section confirm that this is the case. It has been suggested[5,14] that the coherent interaction model[18,19] can account for these results. According to this model, the incident proton interacts collectively with an effective target comprised of the nucleons lying in its path. This effective target is ejected from the nucleus as a single ensemble leaving behind a relatively cold and nearly stationary residue which then deexcites to yield the observed products. Cumming[15] has recently examined the kinematics of this model and derived an expression relating the longitudinal momentum transfer to the mass of the ejected ensemble. In this section we examine the applicability of this formalism to our data.

The reduced longitudinal momentum transfer $\beta q_{\parallel}$ (the convention c=1 is adopted) is related to the mass of the effective target Δm by the expression[15]

$$\beta q_{\parallel} = \Delta E(1+\Delta m/E) \qquad (4)$$

where ΔE is essentially the excitation energy of the residue and E is the total energy of the projectile. This expression predicts that $\beta q_{\parallel}$ should vary linearly with E^{-1}, the intercept being given by ΔE and the slope by $\Delta E \Delta m$.

The results for ^{128}Ba and ^{140}Ba analyzed in this fashion are shown in Fig. 12. In order to increase the number of data points at GeV energies, we have included the results derived from thick-target recoil experiments.[5] It is seen that the results for ^{128}Ba follow the predicted E^{-1} relation above 2 or 3 GeV. By contrast, the two-nucleon collision model,[43] which yields essentially the same relation between momentum transfer and excitation energy as the intranuclear cascade model,[17] predicts a much weaker dependence on E^{-1} in this regime.

The results of a least squares fit to the ^{128}Ba data yield $\Delta E = 67 \pm 14$ MeV and $\Delta m = 27 \pm 6$ amu. These values are rather surprising since Δm is unusually large while ΔE is rather low for a deep spallation process. An evaluation[18] of the probability of finding n nucleons in a tube of cross section σ (the nucleon-nucleon cross section) in a central collision with a heavy element thus indicates that values substantially larger than 10 are highly unlikely. These anomalous results may be merely an indication of the breakdown of the two-step model. The values of $q_{\parallel}$ derived from the data are based on the validity of this model. Although the model has been checked at 2.2 GeV and found to be applicable to the data,[30] it is presently unknown whether this remains the case at the higher energies. If the analysis does turn out to be valid, the data may be an indication of the occurrence of abnormally dense nuclear matter.

The number of nucleons that can be punched out in the primary interaction depends on the nuclear density and an increase in density could thus lead to the observed Δm values. While the occurrence of density isomers has been the subject of much speculation[24-27] there is as yet no definitive evidence that such a process actually happens. The present results suggest that the study of high-energy proton reactions may be fruitful in this respect.

A least-squares fit to the ^{140}Ba data yields $\Delta E=95\pm43$ MeV and $\Delta m=-1.1\pm5.6$. Within the limits of error, the results are identical to those obtained with the two-nucleon collision model. This model, in which the incident proton is reemitted while the struck nucleon is captured ($\Delta m=1$), is expected to be most applicable to the type of peripheral interaction leading to low deposition energy fission.

V. Conclusions

The results obtained for neutron-deficient ^{128}Ba and ^{131}Ba are similar in most respects to those previously reported for Sc fragments from the interaction of ^{238}U with high-energy protons.[10,11] The angular distributions thus change from forward-peaked to sideward-peaked between 3 and 11.5 GeV while the momentum transfer derived from the forward-backward asymmetry approaches zero at the highest energies. The momentum distributions at 0.8 GeV are Gaussians and the values of the mean and the width are indicative of binary fission. With increasing proton energy, the distributions broaden and become asymmetric while the mean momenta decrease sharply, as expected for a deep spallation process. It thus appears that the observed behavior is characteristic of highly inelastic interactions of high-energy protons with heavy elements.

The results obtained up to 3 GeV are consistent with the cascade-evaporation model while at higher energies the results are consistent with the kinematics of the coherent interaction model as derived by Cumming.[15] However, the analysis indicates that 27±6 nucleons are punched out of the nucleus in the coherent interaction, a value that is much larger than realistically expected. To be sure, the analysis is based on the validity of the two-step model and this anomalous result may be merely a reflection of the breakdown of this model. However, the model has been shown to be applicable to the reaction of interest at a bombarding energy of 2.2 GeV[30] and it may well remain applicable at the higher energies. If this proves to be the case, the result may be an indication of the formation of density isomers in central collisions of high-energy protons with heavy elements.

The angular distributions and differential ranges of ^{140}Ba and $^{135}Ba^{m}$ are independent of energy in the GeV regime and indicate that these products are the result of fission following peripheral interactions.

We wish to thank B. J. Dropesky for facilitating the LAMPF irradiations and E. P . Steinberg and S. B. Kaufman for their assistance with the ZGS experiments. The Fermilab experiments were performed in conjunction with similar studies by other groups and we wish to thank N. Sugarman and R. A. Johns for their cooperation. We wish to thank H. Klonk for his participation in the initial phase of this study. This work was financially supported by the U. S. Department of Energy.

References

1. K. Beg and N.T. Porile, Phys. Rev. C3, 1631 (1971).
2. S.B. Kaufman and M.W. Weisfield, Phys. Rev. C11, 1258 (1975).
3. Ø. Scheidemann and N.T. Porile, Phys. Rev. C14, 1534 (1976).
4. S.B. Kaufman, E.P. Steinberg, and M.W. Weisfield, Phys. Rev. C18, 1349 (1978).
5. S. Biswas and N.T. Porile, Phys. Rev. C20, 1467 (1979).
6. L.P. Remsberg and D.G. Perry, Phys. Rev. Lett. 35, 361 (1975).
7. D.R. Fortney and N.T. Porile, Phys. Lett. 76B, 553 (1978).
8. N.T. Porile, S. Pandian, H. Klonk, C.R. Rudy, and E.P. Steinberg, Phys. Rev. C19, 1832 (1979).
9. J.A. Urbon, S.B. Kaufman, D.J. Henderson, and E.P. Steinberg, Phys. Rev. C21, 1048 (1980).
10. D.R. Fortney and N.T. Porile, Phys. Rev. C21, 2511 (1980).
11. D.R. Fortney and N.T. Porile, Phys. Rev. C21, 664 (1980).
12. N.T. Porile, D.R. Fortney, S. Pandian, R.A. Johns, T. Kaiser, K. Wielgoz, T.S.K. Chang, N. Sugarman, J.A. Urbon, D.J. Henderson, S.B. Kaufman, and E.P. Steinberg, Phys. Rev. Lett. 43, 918 (1979).
13. D.R. Fortney and N.T. Porile, submitted to Phys. Rev. C
14. B.D. Wilkins, S.B. Kaufman, E.P. Steinberg, J.A. Urbon, and D.J. Henderson, Phys. Rev. Lett. 43, 1080 (1979).
15. J.B. Cumming, Phys. Rev. Lett. 44, 17 (1980).
16. N.T. Porile and N. Sugarman, Phys. Rev. 107, 1422 (1957).
17. N.T. Porile, Phys. Rev. 120, 572 (1960).
18. G. Berlad, A. Dar, and G. Eilam, Phys. Rev. D13, 161 (1976).

19. Meng Ta-Chung and E. Moeller, Phys. Rev. Lett. 41, 1352 (1978).

20. W. Busza in "High-Energy Physics and Nuclear Structure - 1975" (American Institute of Physics, New York, 1975), p. 211.

21. C. Halliwell, J.E. Elias, W. Busza, D. Luckey, L. Votta, and C. Young, Phys. Rev. Lett. 39, 1499 (1977).

22. J.W. Cronin, H.J. Frisch, M.J. Shochet, J.P. Boymond, P.A. Piroue and R.L. Sumner, Phys. Rev. D11, 3105 (1975).

23. J.P. Vary, K.E. Lassila, and M.S. Sandel, Phys. Rev. C20, 715 (1979).

24. A.B. Migdal, Rev. Mod. Phys. 50, 108 (1978).

25. G.F. Chapline, M.H. Johnson, E. Teller, and M.S. Weiss, Phys. Rev. D12, 4302 (1973).

26. T.D. Lee and G.C. Wick, Phys. Rev. D9, 2291 (1974).

27. V. Ruck, M. Gyulassy, and W. Greiner, Z. Phys. A277, 391 (1976).

28. A.E. Glassgold, W. Heckrotte, and K.M. Watson, Ann. Phys. (New York) 6, 1 (1959).

29. Yu-Wen Yu and N.T. Porile, Phys. Rev. C7, 1597 (1973).

30. V.P. Crespo, J.B. Cumming, and A.M. Poskanzer, Phys. Rev. 174, 1455 (1968).

31. K. Bächmann and J.B. Cumming, Phys, Rev. C5, 210 (1972).

32. C.R. Rudy, N.T. Porile, and S.B. Kaufman, Nucl. Instr. Methods 138, 19 (1976).

33. D.R. Fortney, Ph.D. thesis, Purdue University, 1979 (unpublished).

34. L.C. Northcliffe and R.F. Schilling, Nucl. Data A7, 233 (1970).

35. J. Lindhard, M. Scharff, and H.E. Schiøtt, K. Dan. Videnskab. Selsk. Matt.-Fys. Medd. 33, No. 14 (1963).

36. J. Gosset, H.H. Gutbrod, W.G. Meyer, A.M. Poskanzer, A. Sandoval, R. Stock, and G.D. Westfall, Phys. Rev. C16, 629 (1977).

37. L.P. Remsberg, F. Plasil, J.B. Cumming, and M.L. Perlman, Phys. Rev. 187, 1597 (1969).

38. J.J. Hogan and N. Sugarman, Phys. Rev. 182, 1210 (1969).

39. J.B. Cumming and K. Bächmann, Phys. Rev. C6, 1362 (1972).

40. V.P. Crespo, J.B. Cumming, and J.M. Alexander, Phys. Rev. C2, 1777 (1970).

41. K. Chen, Z. Fraenkel, G. Friedlander, J.R. Grover, J.M. Miller, and Y. Shimamoto, Phys. Rev. 166, 949 (1968).

42. I. Halpern, Nucl. Phys. 11, 522 (1959).

43. A.Turkevich, as quoted by N.T. Porile and N. Sugarman, Phys. Rev. 107, 1410 (1957).

Table I. Parametrization of the angular distributions of Ba products from the interaction of ^{238}U with protons.

Product	Tp (GeV)	A_1	A_2	η_{II}	b/a
^{128}Ba	0.8	0.147±0.020	-0.020±0.026	0.078±0.015	-0.024±0.052
	3.0	0.387±0.015	-0.022±0.017	0.197±0.018	-0.138±0.054
	11.5	0.123±0.011	-0.184±0.011	0.052±0.014	-0.207±0.029
	400	0.064±0.016	-0.234±0.016	0.033±0.026	-0.222±0.022
^{131}Ba	0.8	0.139±0.004	-0.049±0.007	0.072±0.010	-0.069±0.033
	3.0	0.369±0.008	-0.049±0.009	0.172±0.015	-0.091±0.044
	11.5	0.122±0.006	-0.156±0.006	0.057±0.016	-0.188±0.040
	400	0.067±0.011	-0.184±0.015	0.038±0.021	-0.200±0.010
$^{135}Ba^{m}$	0.8	0.106±0.007	-0.065±0.008	0.054±0.010	-0.083±0.034
	3.0	0.035±0.025	-0.052±0.023	0.044±0.032	-0.070±0.108
	11.5	0.070±0.012	-0.013±0.013	0.033±0.021	-0.114±0.200
	400	0.180±0.016	-0.290±0.115	0.046±0.056	-0.540±0.246
^{140}Ba	0.8	-0.001±0.005	-0.217±0.006	0.001±0.013	-0.226±0.040
	3.0	0.019±0.015	-0.189±0.018	0.016±0.028	-0.281±0.078
	11.5	0.001±0.000	-0.150±0.000	0.000±0.015	-0.197±0.028
	400	0.033±0.011	-0.200±0.013	0.019±0.015	-0.217±0.019

Table II. Quantities derived from 90^{o} differential ranges.

Product	Tp (GeV)	<P> $(MeV \cdot A)^{\frac{1}{2}}$	FWHM $(MeV \cdot A)^{\frac{1}{2}}$	<T> (MeV)	$\langle v_{II} \rangle$ $(MeV/A)^{\frac{1}{2}}$
^{128}Ba	0.8	120±3	40±16	59.1±3.2	0.067±0.013
	3.0	83.6±2.3	100±20	31.6±1.9	0.103±0.009
	11.5	68.2±1.4	110±20	22.1±1.2	0.022±0.006
	400	66.1±1.4	80±15	20.6±1.1	0.014±0.001
^{131}Ba	0.8	121±2	38±5	57.7±2.9	0.062±0.008
	3.0	88.9±2.0	100±30	34.9±1.9	0.093±0.008
	11.5	74.4±1.5	130±30	26.0±1.3	0.024±0.007
	400	70.8±1.5	132±30	23.5±1.2	0.016±0.009
$^{135}Ba^{m}$	0.8	137±3	33±9	71.6±3.8	0.053±0.010
	3.0	122±3	48±9	57.0±3.0	0.038±0.028
	11.5	125±3	35±9	59.0±3.0	0.029±0.019
	400	127±4	40±8	60.1±4.3	0.042±0.033
^{140}Ba	0.8	139±3	28±2	69.2±3.5	0.001±0.013
	3.0	141±3	34±7	71.6±3.7	0.016±0.027
	11.5	140±3	31±7	71.1±3.6	0.000±0.016
	400	142±3	26±2	72.3±3.7	0.019±0.015

Figures

Fig. 1. Angular distributions of ^{128}Ba from the interaction of ^{238}U with 0.8-400 GeV protons. The points represent the averages of replicate determinations. The curves are the result of a two-step model fit as given by Eq. (1).

Fig. 2. Angular distributions of ^{131}Ba from the interaction of ^{238}U with 0.8-400 GeV protons. See Fig. 1 for details.

Fig. 3. Angular distributions of ^{140}Ba from the interaction of ^{238}U with 0.8-400 GeV protons. See Fig. 1 for details.

Fig. 4. Momentum distribution of ^{128}Ba fragments emitted at 90^{o} in the interaction of ^{238}U with 0.8-400 GeV protons. The different symbols correspond to results obtained in replicate experiments. The curve at 0.8 GeV is the result of a Gaussian fit; at the higher energies the curves are drawn to guide the eye.

Fig. 5. Momentum distribution of ^{131}Ba fragments emitted at 90^{o} in the interaction of ^{238}U with 0.8-400 GeV protons. See Fig. 4 for details.

Fig. 6. Momentum distribution of $^{135}Ba^{m}$ fragments emitted at 90^{o} in the interaction of ^{238}U with 0.8-400 GeV protons. See Fig. 4 for details; note that the curves are Gaussian fits at all energies.

Fig. 7. Momentum distribution of ^{140}Ba fragments emitted at 90^{o} in the interaction of ^{238}U with 0.8-400 GeV protons. See Fig. 6 for details.

Fig. 8. Energy dependence of mean fragment momentum. The various symbols correspond to the different Ba isotopes: ●, ^{128}Ba; Δ, ^{131}Ba; ○, $^{135}Ba^{m}$; ▲, ^{140}Ba. The points at 2.2 GeV are from refs. 30 and 31.

Fig. 9 Energy dependence of full width at half-maximum of Ba momentum distributions. See Fig. 8 for details.

Fig. 10. Energy dependence of anisotropy parameter b/a. See Fig. 8 for details.

Fig. 11. Energy dependence of mean forward component of velocity of struck nuclei leading to Ba formation. See Fig. 8 for details.

Fig. 12. Dependence of reduced longitudinal momentum on reciprocal of the total energy of incident proton. Open points, present data; closed points, based on thick-target recoil data [ref. 5]. The solid lines are results of least squares fits; the dashed lines represent the dependence predicted by the two-nucleon collision model.

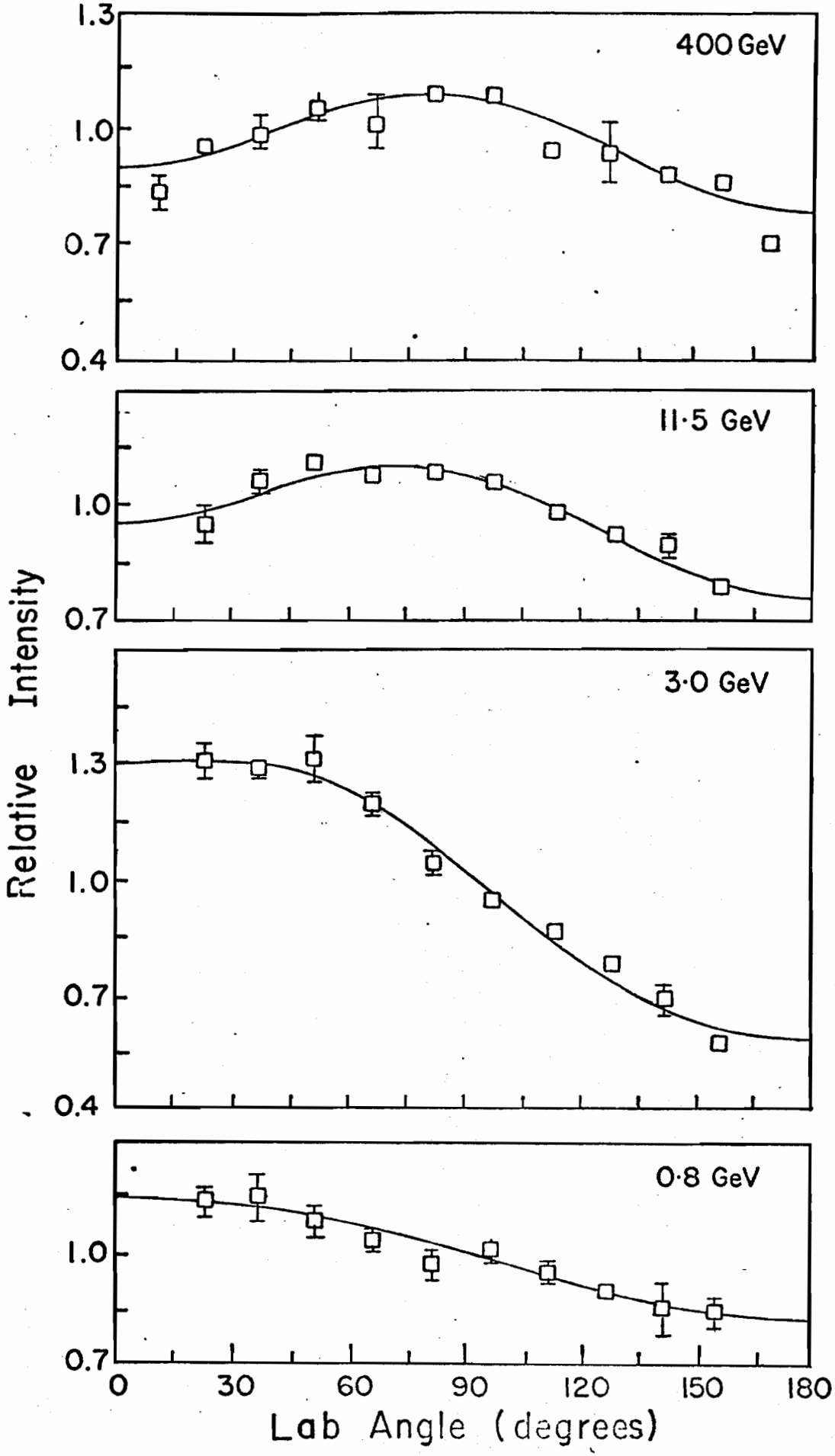

Pandian's Paris Fig. 1

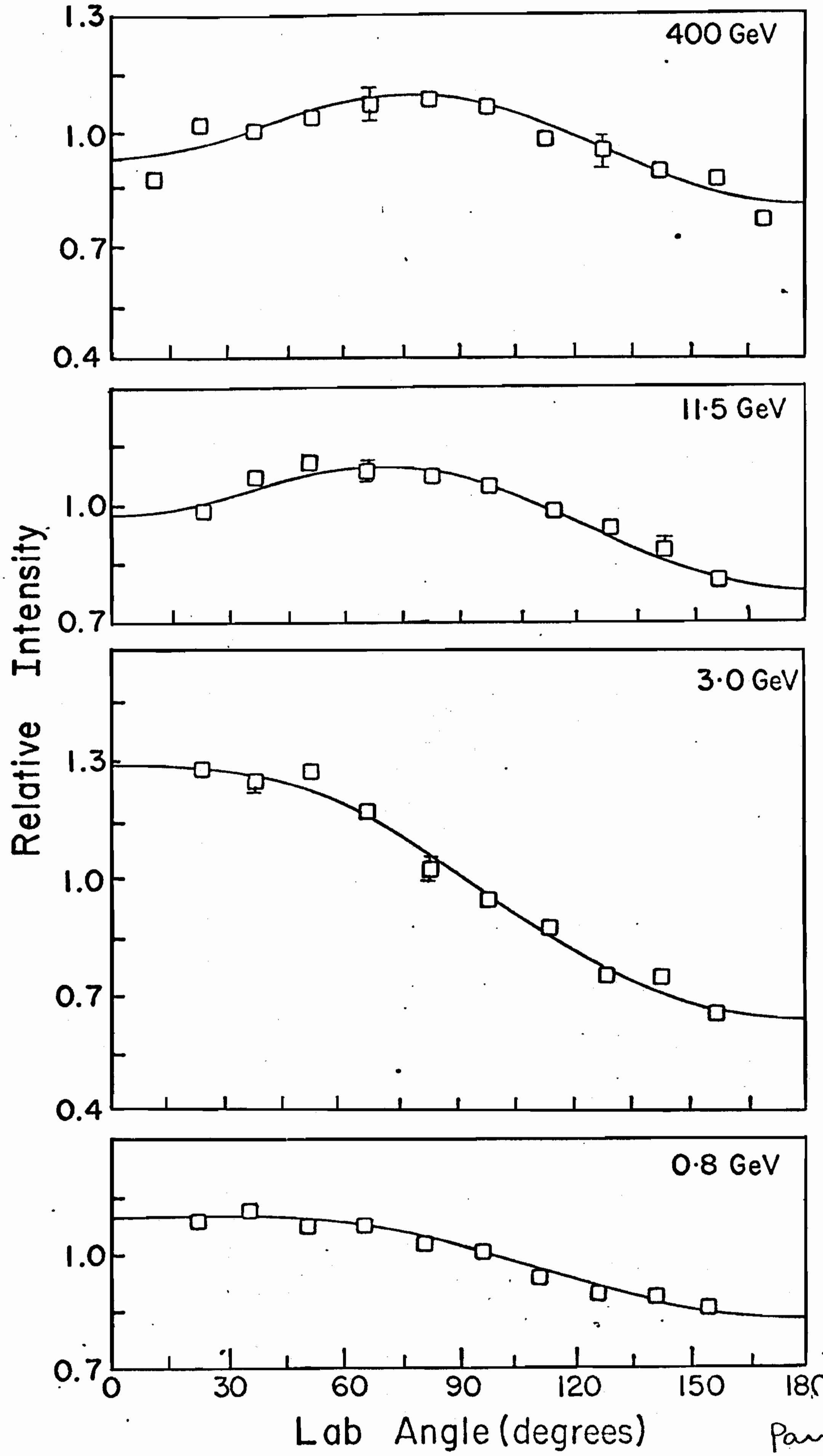

Pandian & Pil... Fig ~

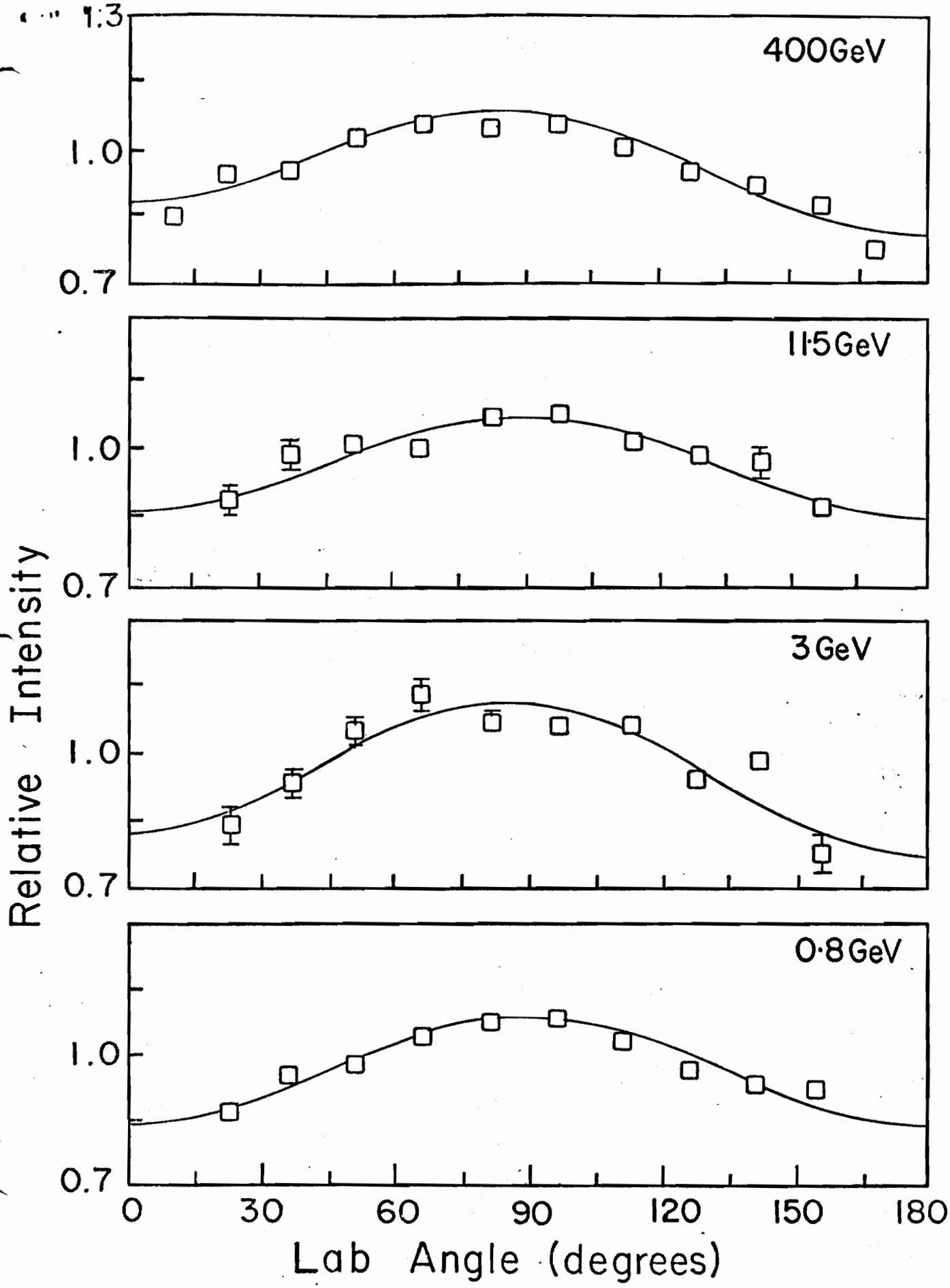

Pandian & Parle
Fig. 3

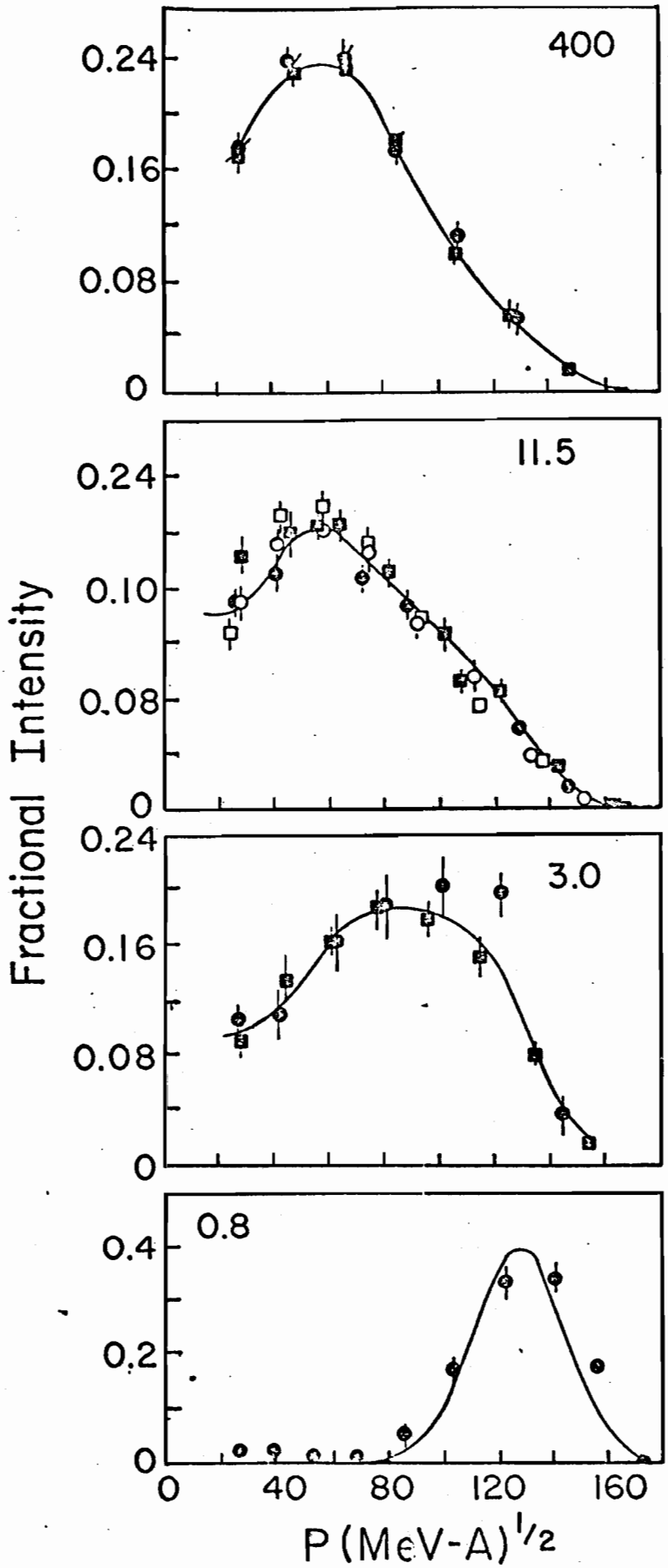

Pandian & Prill
Fig. 4

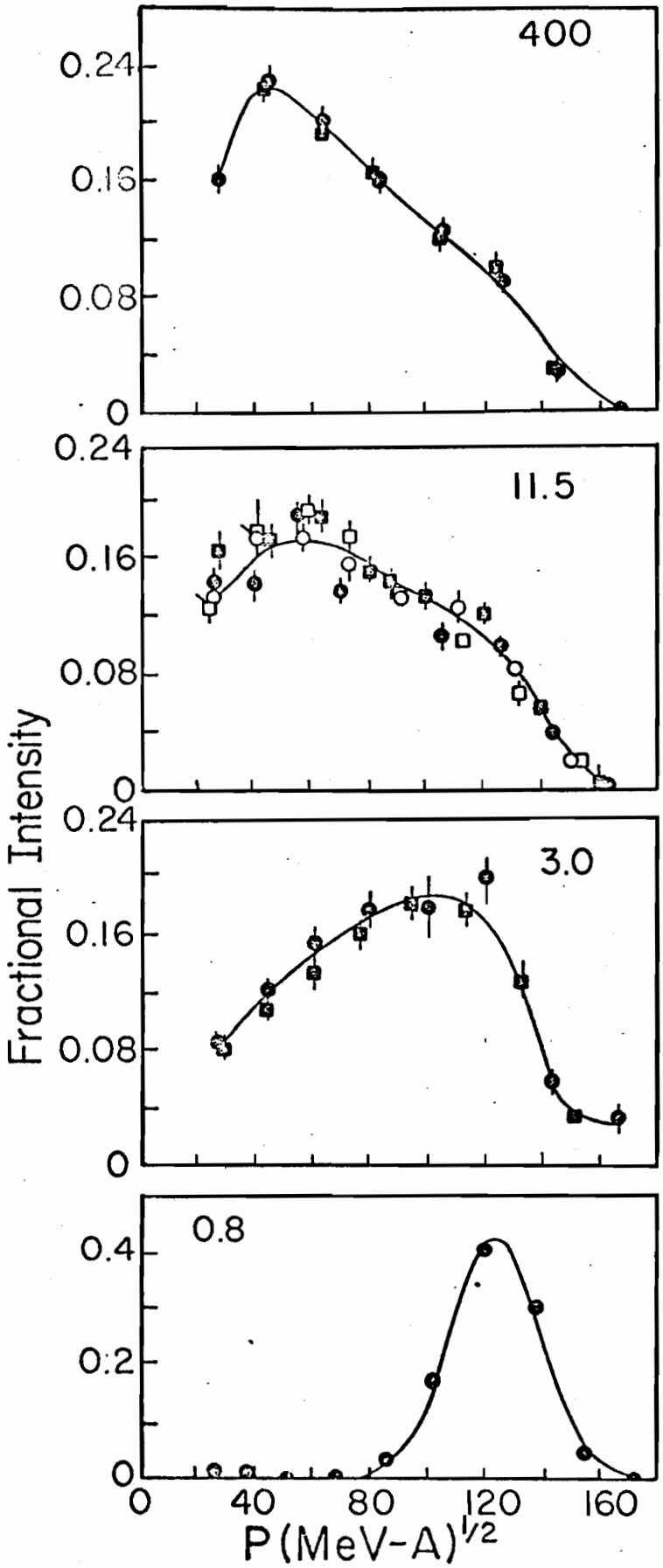

• Pandian to Parile
Fig. 5

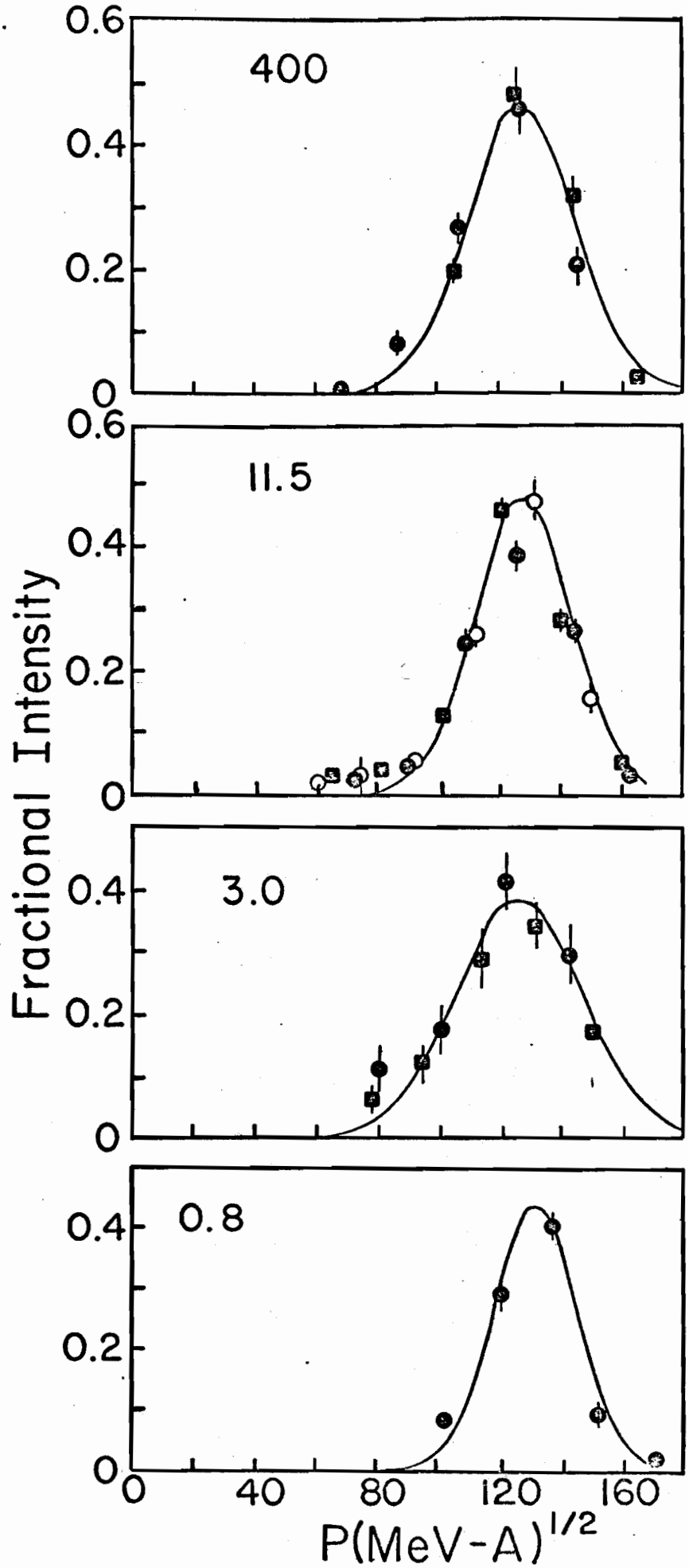

Parodian & Poirle
Fig. 6

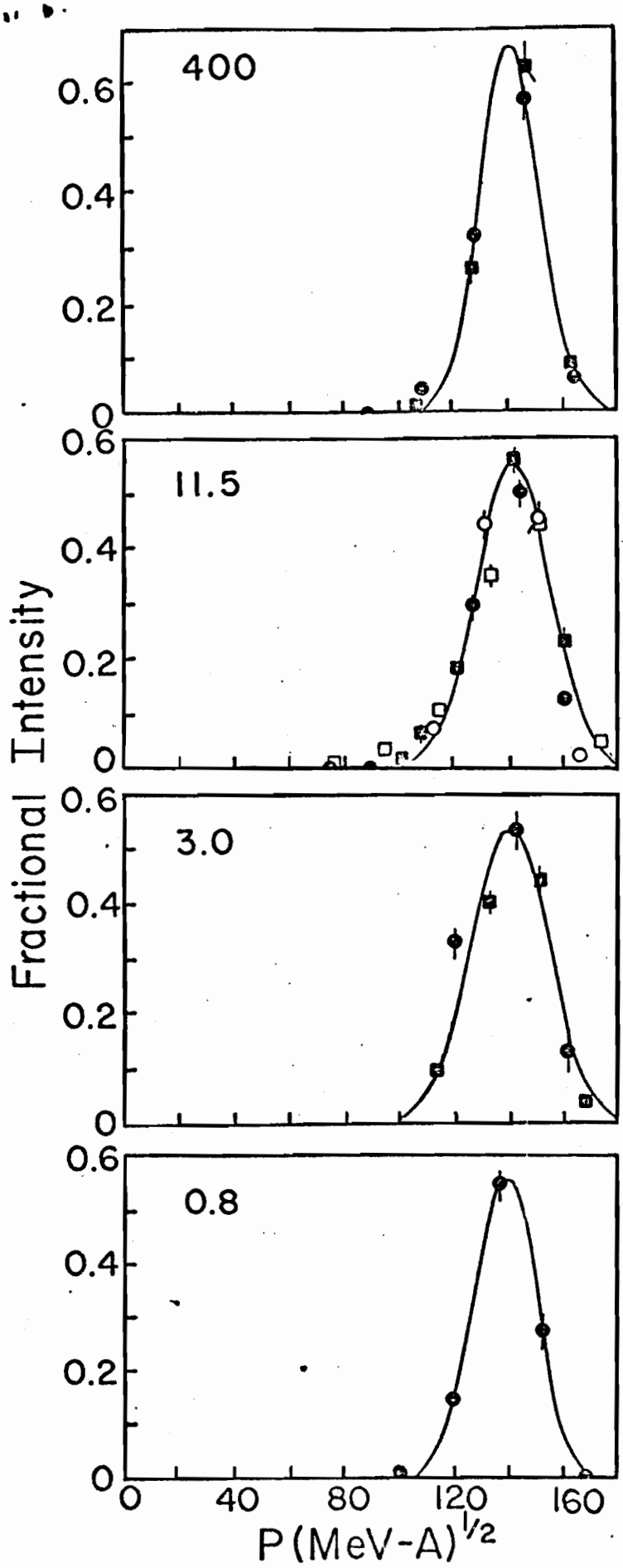

Pandian & Parikh
Fig. 7

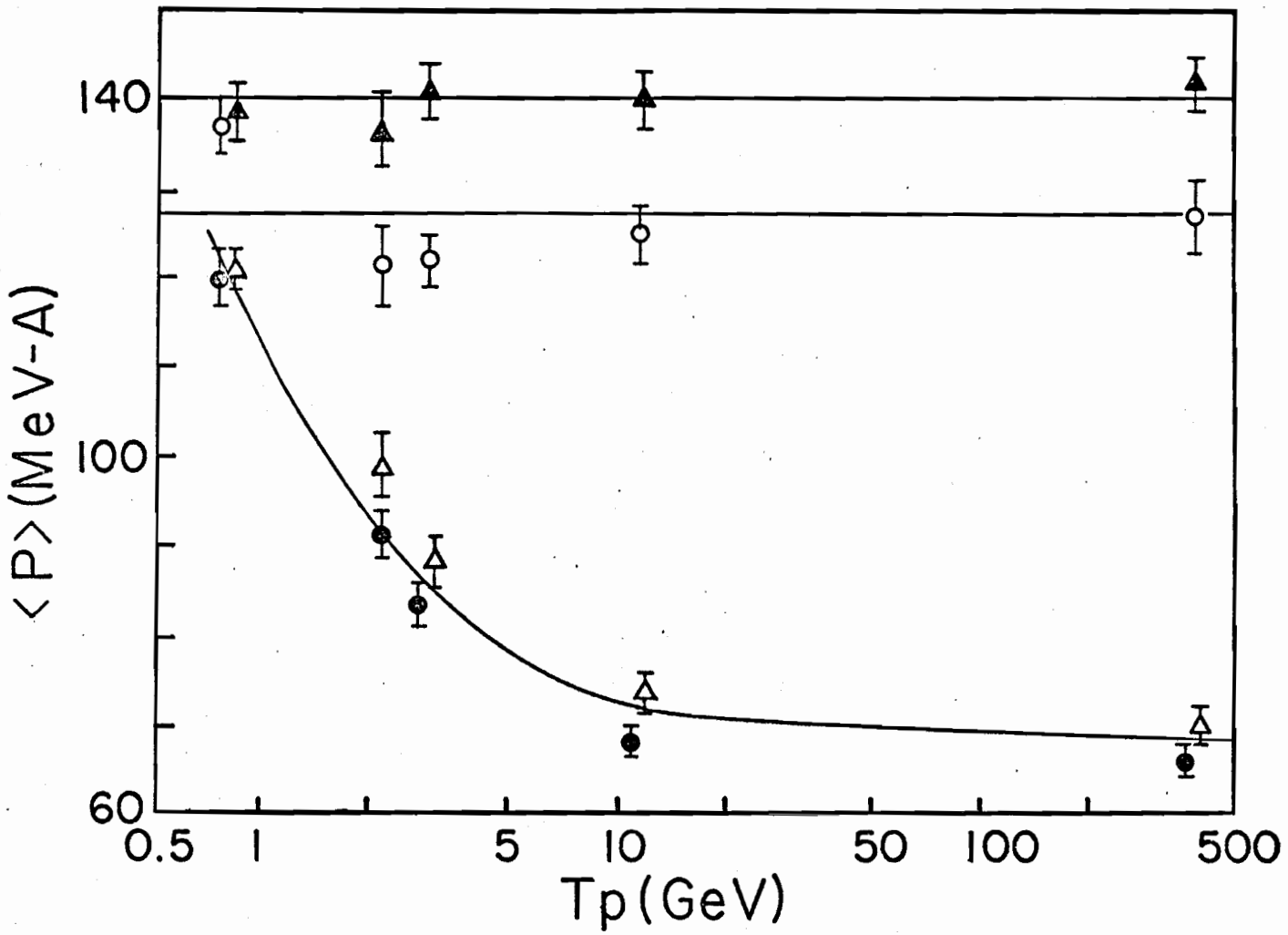

Pandion o Pion's
Fig. 8

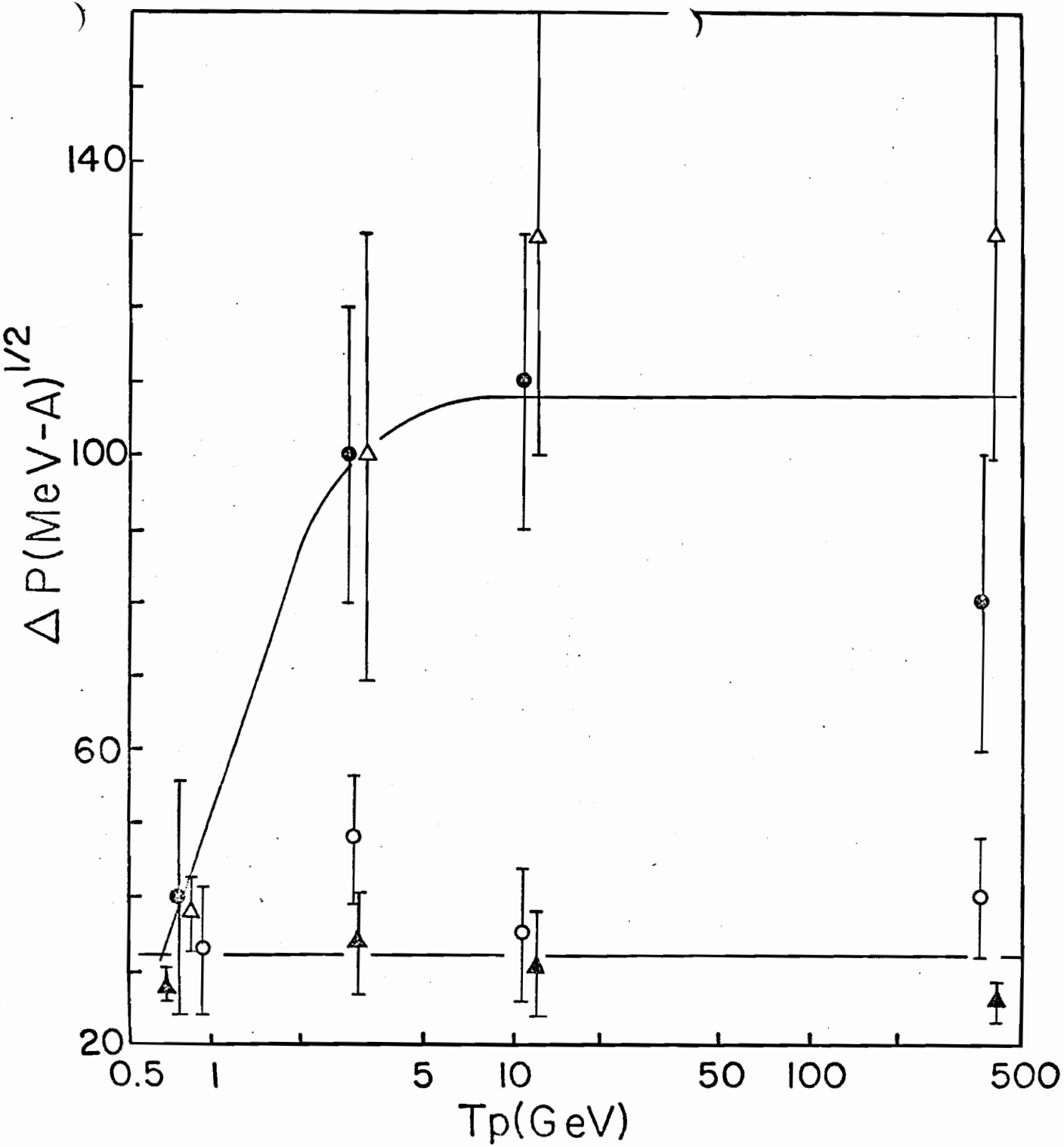

Pandian to Pais
Fig. 9

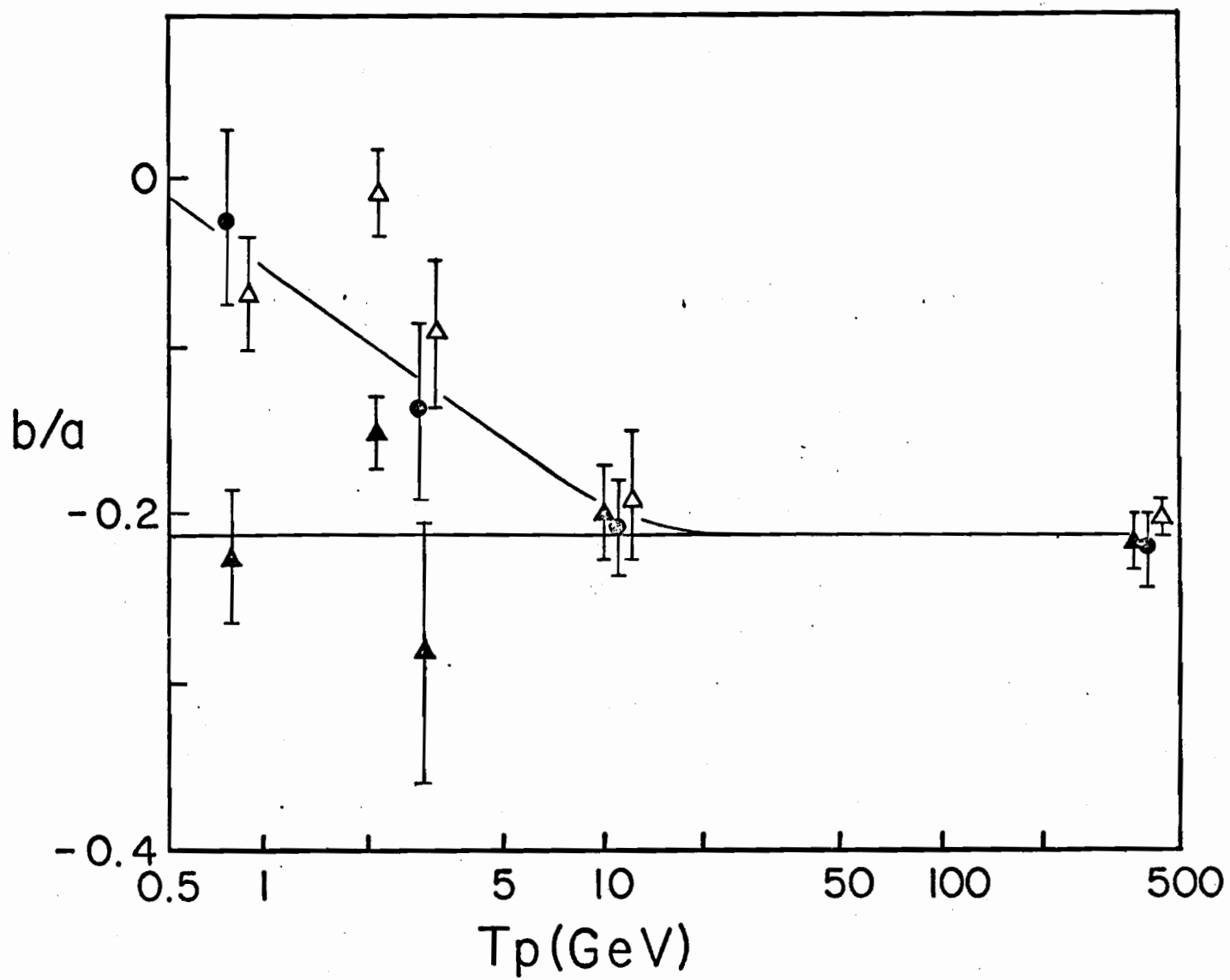

Pandian & Peirce
Fig. 10

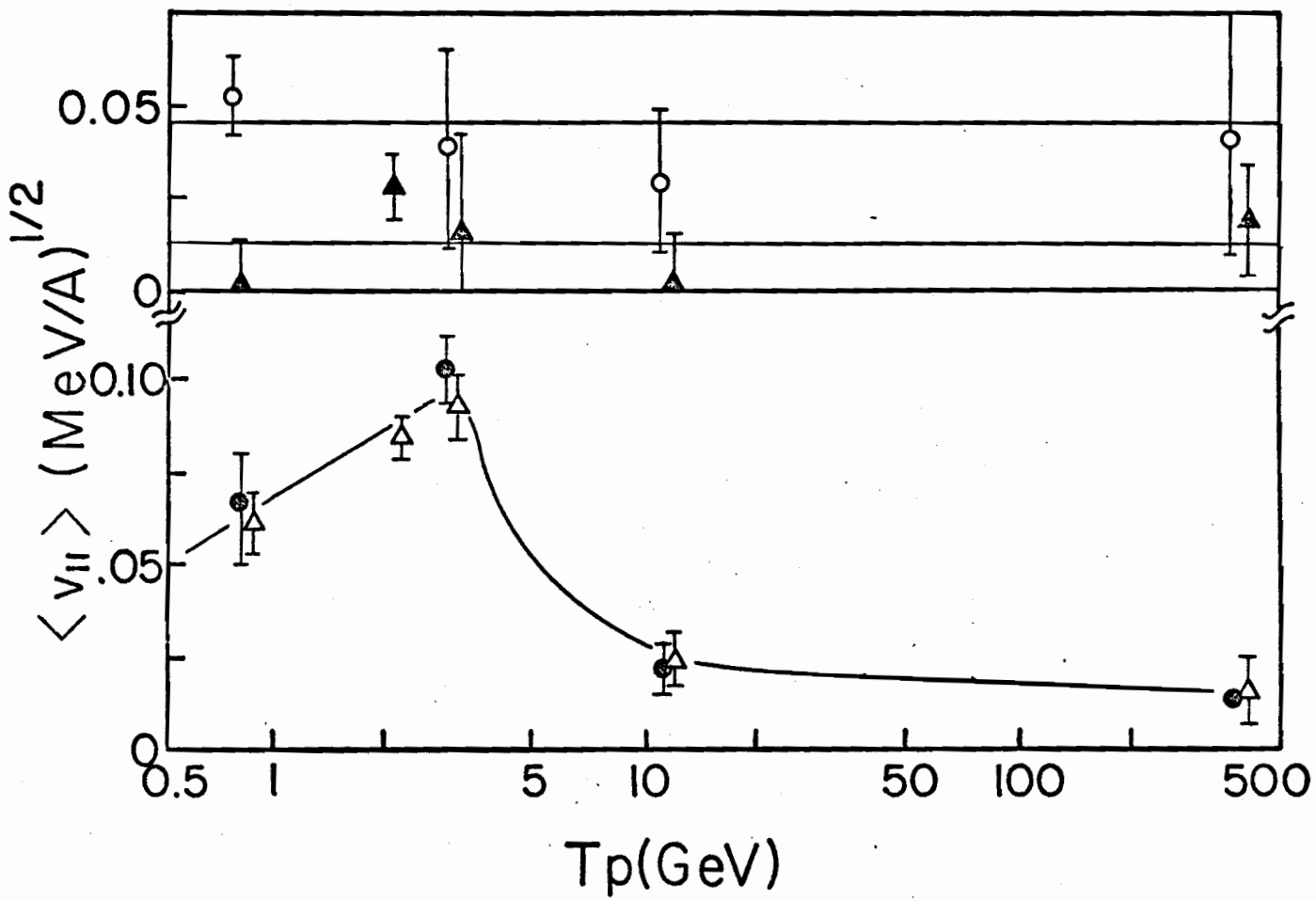

Paulian b Pauls
Fig. 11

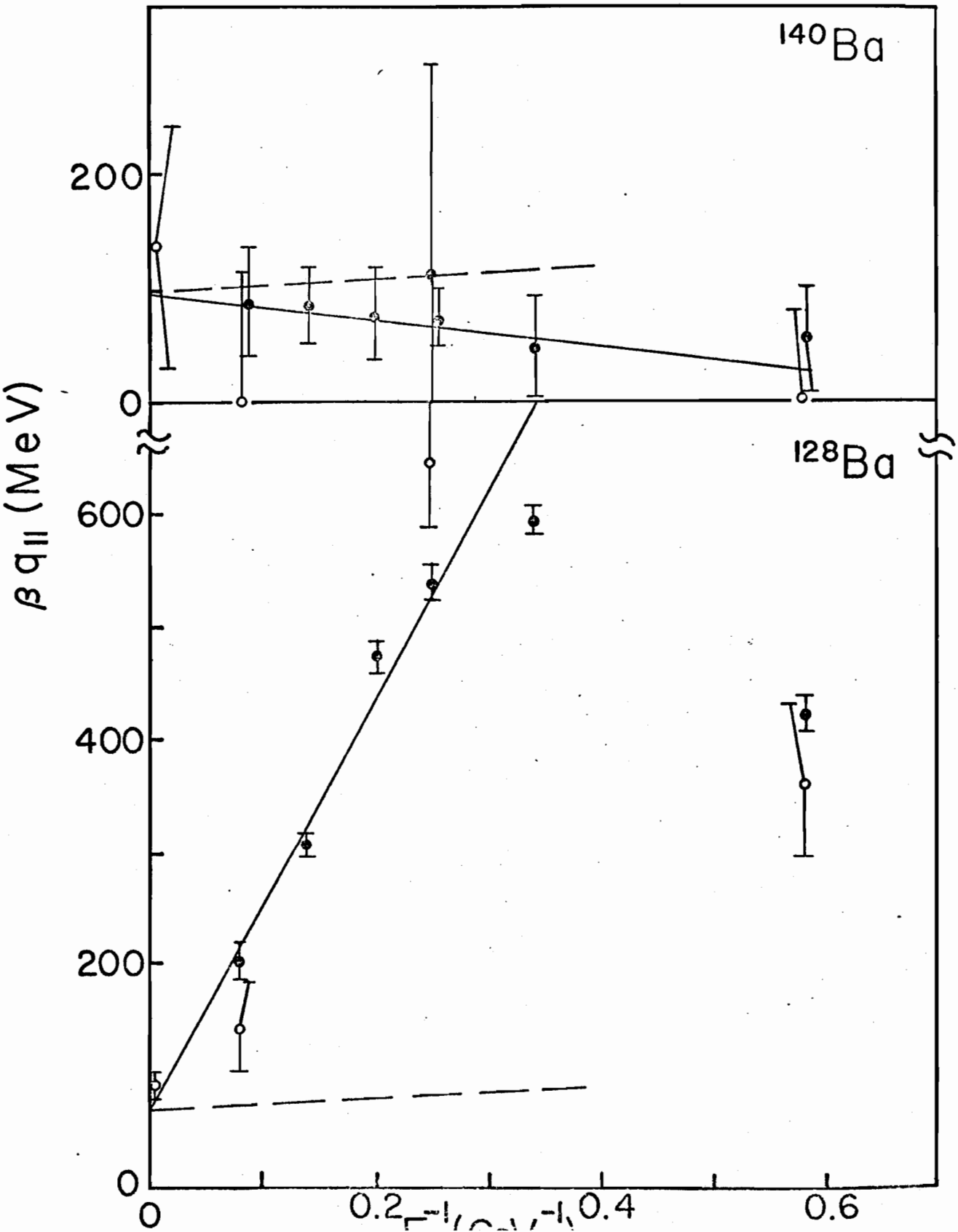
^{140}Ba
^{128}Ba
200
0
600
400
200
0
βq_{II} (MeV)
0
0.2
0.4
0.6